Relative Input Strength Rapidly Regulates Dendritic Structure of Chick Auditory Brainstem Neurons

Staci A. Sorensen[1] and Edwin W. Rubel[2]*

[1]Allen Institute for Brain Science, Seattle Washington 98113
[2]University of Washington, Seattle, Washington 98195-7923

ABSTRACT

Competition between presynaptic inputs has been suggested to shape dendritic form. This hypothesis can be directly tested on bitufted, auditory neurons in chicken nucleus laminaris (NL). Each NL neuron contains two relatively symmetrical dendritic arbors; the dorsal dendrites receive excitatory glutamatergic input from the ipsilateral ear, and the ventral dendrites receive corresponding input from the contralateral ear. To assess the effect of relative synaptic strength on NL dendrites, we used single-cell electroporation; electrophysiology; and live, two-photon laser scanning microscopy to manipulate both the amount and the balance of synaptic input to the two matching sets of dendrites. With simultaneous activation, both sets of dendrites changed together, either growing or retracting over the imaging period. In contrast, stimulation of only one set of dendrites (either dorsal or ventral) resulted in the unstimulated dendrites losing total dendritic branch length, whereas the stimulated dendrites exhibited a tendency to grow. In this system, balanced input leads to balanced changes in the two sets of dendrites, but imbalanced input results in differential changes. Time-lapse imaging revealed that NL dendrites respond to differential stimulation by first decreasing the size of their unstimulated dendrites and then increasing the size of their stimulated dendrites. This result suggests that the relative activity of presynaptic neurons dynamically controls dendritic structure in NL and that dendritic real estate can rapidly be shifted from inactive inputs to active inputs. J. Comp. Neurol. 519:2838–2851, 2011.

INDEXING TERMS: dendrites; activity; competition; auditory; time-lapse imaging

Activity-dependent competition between neuronal inputs has been suggested to play an important role in nervous system development. By this mechanism, communication between pre- and postsynaptic neurons facilitates the maintenance of active presynaptic inputs and the elimination of less active inputs. This process suggests that the pattern of activation, rather than the presence or absence of input, is most important for regulating synaptic strength. This mechanism has been particularly well studied in the establishment of neuromuscular synapses (Balice-Gordon and Lichtman, 1994; Lichtman and Colman, 2000; Personius and Balice-Gordon, 2001) and cortical and cerebellar connections (Hashimoto et al., 2009; Hata et al., 1999; Hua et al., 2005; Katz and Shatz, 1996). Much work has been done to understand how the presynaptic axons are affected by the relative activity of neighboring inputs, but the effect on the dendritic processes is not well understood.

The third-order nucleus of the chicken auditory system, nucleus laminaris (NL), provides a useful model system in which to address questions about the effect of synaptic input on the structure of individual dendrites. Specifically, NL neurons have two sets of relatively symmetrical dendrites, a dorsal and a ventral domain (Deitch and Rubel, 1984; Smith, 1981; Smith and Rubel, 1979). Segregated inputs from nucleus magnocellularis (NM) provide each set of dendrites with excitatory information from one ear; ipsilateral and contralateral NM axons form synapses with the dorsal and ventral dendrites, respectively. The convergence of inputs from the two ears allows NL neurons to function as coincidence detectors in a neuronal circuit involved in sound localization (Carr and Konishi, 1990). For our purposes, it also allows us to selectively

Grant sponsor: National Instituite of Deafness and Other Communication Disorders; Grant number: DC03829; Grant number: DC07008; Grant number: DC04661.

*CORRESPONDENCE TO: Edwin W. Rubel, University of Washington, Box 357923, Seattle, WA 98195-7923. E-mail: rubel@u.washington.edu

Received August 23, 2010; Revised March 6, 2011; Accepted April 5, 2011
DOI 10.1002/cne.22656
Published online April 15, 2011 in Wiley Online Library (wileyonlinelibrary.com)

manipulate excitatory input to one or both of the matching sets of dendrites

Previous in vivo work demonstrated that dendrites in NL, and the mammalian medial superior olivary nucleus (MSO), depend on afferent input for their development (Feng and Rogowski, 1980; Parks, 1981; Parks et al., 1987; Russell and Moore, 1999) and maintenance (Benes et al., 1977; Deitch and Rubel, 1984, 1989). More recent work demonstrated that glutamatergic input maintains NL dendrite length in vitro and that the pattern, not the absolute amount, of glutamatergic synaptic input regulates NL dendrite structure. Specifically, stimulation of the dorsal dendrites led to growth of stimulated dendrites and retraction of the unstimulated dendrites on the opposite side of the cell, suggesting that NM inputs might compete for synaptic space on NL dendrites.

The current experiments used electrophysiology and time-lapse, two-photon laser scanning microscopy to test the hypothesis directly. By employing multiple stimulation conditions, we found that relative input strength regulates the relative size of the two NL dendritic arbors on a very short time scale; stimulation of *either* dorsal or ventral dendrites resulted in decreased dendritic length in the unstimulated dendrites and growth of the stimulated dendrites. Time course studies demonstrated that NL dendrites responded to differential stimulation by first decreasing the size of their inactive dendrites and then increasing the size of their active dendrites. In contrast, bilaterally stimulated and unstimulated, control dendrites either grew or retracted together over the imaging period. These data indicate that balanced input maintains the relative sizes of the two sets of NL dendrites, and unbalancing these inputs leads to rapid, input-specific changes in dendritic structure.

MATERIALS AND METHODS

Slicing procedures

Acute brainstem slices were made from white leghorn chicken embryos, at embryonic day 14–19 as previously described (Monsivais et al., 2000). At this age, chicks have functional hearing (Rebillard and Rubel, 1981; Saunders et al., 1974), but the dendrites (Rubel et al., 1981) and electrical properties (Gao and Lu, 2008) of NL neurons are still developing. Embryos were removed from the egg and rapidly decapitated. The brainstem was quickly dissected out into room temperature oxygenated artificial cerebral spinal fluid (ACSF; 130 mM NaCl, 2.5 mM KCl, 1.25 NaH_2PO_4, 26 mM $NaHCO_3$, 1 mM $MgCl_2$, and 2 mM $CaCl_2$ in filtered dH_2O) and blocked for further sectioning. Coronal sections were then cut at 400 μm thickness using a vibratome (Technical Products International, St. Louis, MO). Vibratome sections were placed in a slice chamber containing oxygenated ACSF heated to 34–36°C and allowed to equilibrate for 30 minutes to 1 hour. The University of Washington animal care committee approved all procedures.

Electroporation procedures

After equilibration, slices were transferred to a Leica MZFLIII fluorescent dissecting microscope (Leica, Northvale, NJ), and individual NL neurons were filled with anionic tracer using a method for single-cell electroporation adapted from Haas et al. (2001) and described in detail by Sorensen and Rubel (2006). Briefly, slices were placed in a Sylgard-coated chamber containing oxygenated ACSF and a reference electrode. A stimulating electrode containing anionic tracer was positioned on the surface of the slice within the line of NL cell bodies. An Electro Square Porator (model ECM 830; BTX, San Diego, CA) was used to apply a voltage (25–40 V, 50 msec duration, train of two to eight pulses) to the slice. This procedure instantaneously labeled the cell body and dendrites of single NL neurons. For these experiments, we used a solution of 5–10% Alexa 594 dextran (Molecular Probes, Eugene, OR) in sterile saline to label one or two NL cells on both sides of the slice. After electroporation, slices were briefly returned to the holding chamber, before being transferred to the multiphoton microscope described below.

Imaging procedures

Slices were kept alive during imaging experiments by continual perfusion with oxygenated ACSF (perfusion ACSF contained 3 mM $CaCl_2$) warmed with an in-line solution heater (model SF-28; Warner Instruments, Hamden, CT) to 34°C. Digital images of NL cells were captured with a Zeiss 510 Multi-Photon NLO microscope system coupled to a Zeiss Axiovert 200 stand using AIM for LSM510 scanning control software (LSM 510 MP-NLO; Carl Zeiss Microimaging). The light source used was a Coherent Mira 900 titanium:sapphire femtosecond pulse laser. All cells were imaged with a Plan Neofluar ×40 oil immersion objective (NA 1.3, 0.12 mm working distance). Images were acquired once per hour for up to 5 hours. Imaging parameters varied with the tenfold change in dendritic length along NL's tonotopic map (Smith and Rubel, 1979). Neurons taken from the high-frequency region of the nucleus have smaller dendrites and could be imaged with a higher resolution (0.17–0.25 μm/pixel) than neurons taken from the low-frequency region of the nucleus, where the dendrites are much larger (0.26–0.45 μm/pixel). When possible, neurons from the middle region of the nucleus were studied. For images acquired

at the beginning (0 hours) and the end of experiments (final hour), a z-series of 100–200 consecutive images (with a distance of 0.4–0.5 μm between images) was taken through the entire extent of the neuron (512 × 512). For images acquired at the intervening time points, only NL dendrites (and not their cell bodies) were imaged using the region of interest tool in the LSM software. All images shown are Z-stack projections. For qualitative comparison of dendrites across time points, images were first split into dorsal and ventral regions, and then aligned to the cell body and/or to the base of the primary dendrites. When images of the two time points are presented together, the same image adjustment parameters in Adobe Photoshop 7.0 were used for both time points. Whole-cell images are not shown because changes in the cell body throughout the imaging period did not allow both sets of dendrites to be aligned in the same image.

In vitro physiological stimulation and recording procedures

Selective stimulation of the dorsal or ventral dendrites.

To stimulate the dorsal dendrites of NL neurons selectively, a concentric, bipolar stimulating electrode (FHC, Bowdoinham, ME) was placed on NM ipsilateral to the NL neuron being imaged (see schematic in Fig. 2A). To stimulate the ventral dendrites of NL neurons selectively, a concentric, bipolar stimulating electrode (FHC) was placed on NM contralateral to the NL neurons being imaged (see schematic in Fig. 3A). An A-M Systems 2100 Isolated Pulse Stimulator was used to apply voltage pulses of 10–20 V and 1 msec duration at 10–25 Hz for 4–5 hours. Borosilicate recording electrodes filled with 1 M NaCl (1–10 MΩ) were used to confirm the effect of the stimulation throughout the experiment. The recording electrode was placed in the lateral portion of NL, ipsilateral to the neuron being imaged. This recording electrode position was used for all the stimulation experiments described here. NL neurons were imaged only in slices in which postsynaptic field potentials were confirmed. The strength of the stimulus was adjusted throughout the experiment such that the strongest possible field potential could be recorded. The postsynaptic component of the field potential was determined in separate experiments by blocking with 0.1 M DNQX and 0.1 M AP-5.

Bilateral stimulation of both sets of NL dendrites.

To activate both sets of NL dendrites simultaneously, two stimulating electrodes (described above) were placed on the brainstem, one on NM on each side of the slice (see schematic in Fig. 4A). For these experiments, the contribution of the ipsilateral and contralateral NM nuclei was confirmed at the beginning of the experiment by demonstrating that each stimulating electrode alone could elicit a postsynaptic field potential.

Three-dimensional morphological analysis procedures

Huygens Essential software was used to deconvolve each image stack (version 2.7.3p3; Scientific Volume Imaging B.V., Hilversum, The Netherlands). Deconvolved stacks were then imported into Object Image 2.11, and a series of substack projections was made to create image stacks for analysis with an effective z-step of ~1 μm. Analyzed image stacks consisted of 30–80 images.

In Object Image, the dorsal and ventral dendrites of each neuron were separately analyzed in each 3D z-stack for either the total dendritic branch length (TDBL) or length of individual dendritic branches and branch dynamics. It is important to note that, for all images, the experimenter was blind to the imaging time point and the type of dendrite being analyzed (dorsal vs. ventral and stimulated vs. unstimulated). The macros used for these analyses were kindly provided by Hollis Cline's laboratory (http://clinelab.cshl.edu/methods.html).

For branch length and dynamics analyses, the z-stacks from each time point were opened simultaneously. Within the z-stack, a single dendritic branch was chosen and then located (if present) in all other z-stacks. Within each z-stack, a line was then drawn through the center of the dendrite from its terminal tip through each successive z-section to its origin at the cell body or parent dendrite. All individual dendritic branches from each cell were analyzed in this way. If any individual dendrite was cut off in any plane, or at any time point, it was not included in the analysis. Z-axis rotations were routinely made to confirm that dendrites were not cut off in this plane. Each dendrite was assigned a number, which allowed us to track changes in the length of individual dendritic branches across imaging time points. By summing individual branch lengths at each time point, changes in the total dendritic branch length (TDBL) of the whole dendritic tree could be calculated. For each neuron, TDBL was measured separately for dorsal and ventral dendrites. Thus, each neuron had two measures of TDBL at each time point. The mean dorsal TDBL and ventral TDBL for each group were then calculated at each time point. For all cells, the percentage change in TDBL was compared between the initial and the final time points. Quantitative comparisons between TDBL changes for an entire set of dendrites and TDBL for only 60 of the neuron's dendrites indicated that there was little difference between the changes detected with

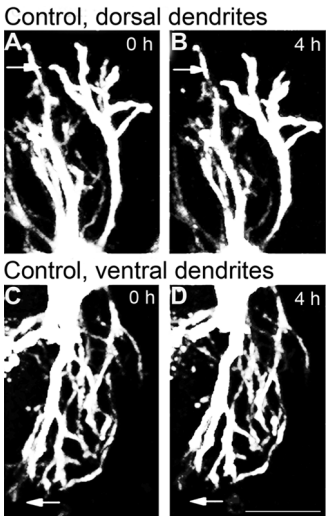

Figure 1. Representative example of unstimulated, control dorsal (**A,B**) and ventral (**C,D**) dendrites from one NL neuron imaged at 0 and 4 hours. Images at left were taken at 0 hours. The same dendrites imaged 4 hours later are shown at right. Both sets of dendrites remained fairly stable between the imaging periods, but several branches can be observed to retract between the imaging periods (arrows). Scale bar = 20 μm.

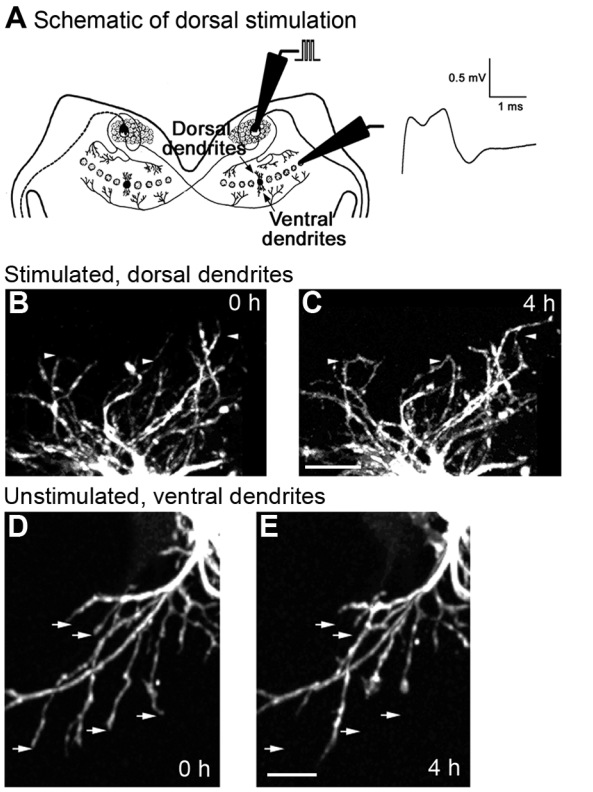

Figure 2. Schematic of the dorsal-only stimulation paradigm (**A**). A bipolar stimulating electrode was placed in NM ipsilateral to the NL neuron being imaged (arrows). Field potentials (averaged and shown at right) were recorded from the lateral portion of NL. With this configuration, only the dorsal dendrites, and not the ventral dendrites, were activated. Examples of stimulated dorsal (**B,C**) and unstimulated ventral (**D,E**) NL dendrites. Images at left were taken at 0 hours. The same dendrites imaged 4 hours later are shown at right. Several branches of the stimulated, dorsal dendrites grew between the imaging time points (B,C), while many branches of the unstimulated ventral dendrites retracted (D,E). Scale bar = 25 μm.

the two measurements (data not shown). Thus, for some neurons, only a subset of the dendrites was measured and included in the analysis of TDBL. We also compared the percentage difference between the initial TDBL and the TDBL at each subsequent time point for control, bilateral, and dorsal-only stimulation of neurons. To be considered branch growth or retraction, the change between the initial length measurement and the measurement at a subsequent time point had to be at least 10%. Using this threshold, the mean percentage of branches that grew, retracted, or remained stable (within 10% of their original length) at each time point was also compared. These percentages add up to 100%. Statview (SAS institute Inc., Cary, NC) was used for statistical analyses. Significance was determined by using an ANOVA and individual Fischer's PLSD test; $P < 0.05$ was considered statistically significant. Unless otherwise noted, all data are shown as mean ± SE.

For these experiments, five control neurons and four bilateral stimulation neurons were analyzed, for a total of 312 control dendritic branches and 270 bilaterally stimulated dendritic branches. For ventral stimulation experiments, seven neurons were used, for a total of 415 dendritic branches. For dorsal stimulation experiments, four neurons were used, for a total of 189 dendritic branches. For all experiments, electroporated NL neurons that exhibited aberrant changes in morphology were not included in our analyses.

RESULTS

We examined the effect of different electrophysiological stimulation conditions on the two sets of dendrites of single dye-filled NL neurons in vitro using time-lapse, multiphoton imaging. For these experiments, NL neurons were imaged before stimulation began (0 hours) and then once per hour for 4–5 hours during stimulation of the dorsal and/or ventral dendrites (see schematic in Figs. 2A, 3A for example physiological traces). For comparison, we also imaged unstimulated control neurons using these same imaging parameters. In the absence of external stimulation, these slices do not fire spontaneous action potentials. Figures 1–4 show representative z-projection images of control, dorsal-only, ventral-only, and bilaterally stimulated NL neurons at the 0 and 4–5 hours imaging

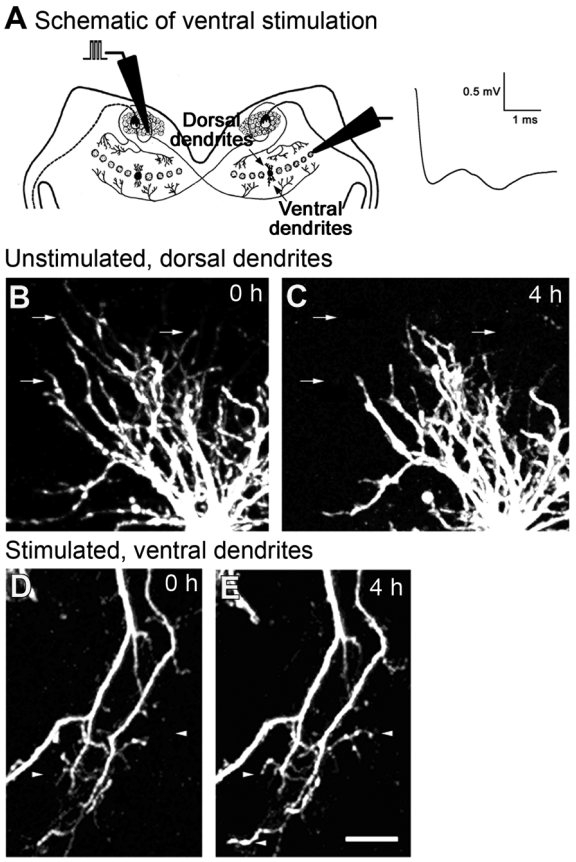

Figure 3. Schematic of the ventral-only stimulation paradigm (**A**). A bipolar stimulating electrode was placed in NM contralateral to the NL neuron being imaged (arrows). Field potentials (averaged and shown at right) were recorded from the lateral portion of NL. With this configuration, only the ventral dendrites, and not the dorsal dendrites, are activated. Examples of unstimulated dorsal (**B,C**) and stimulated ventral (**D,E**) NL dendrites. Images at left were taken at 0 hours. The same set of dendrites imaged 4 hours later is shown at right. Several branches of the unstimulated dorsal dendrites lost length between the imaging time points (B,C), while several branches of the stimulated ventral dendrites grew (D,E). Scale bar = 25 μm.

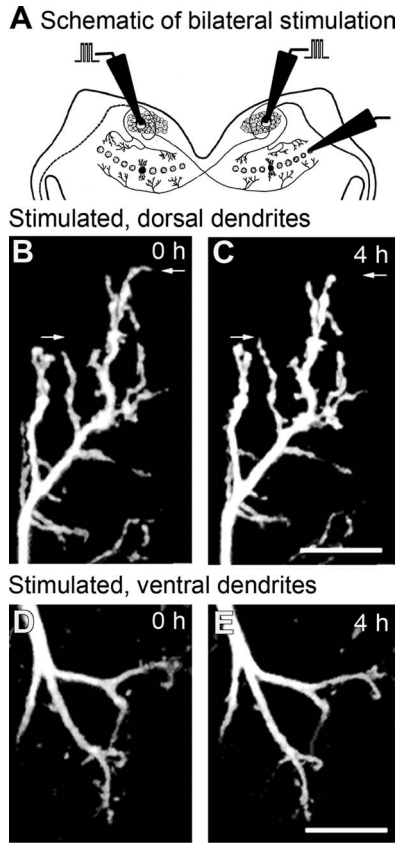

Figure 4. Schematic of the bilateral stimulation paradigm (**A**). A bipolar stimulating electrode was placed in NM on each side of the slice. Field potentials were recorded from the lateral portion of NL on one side of the slice. With this configuration, both the dorsal and the ventral dendrites are activated. Representative example of bilaterally stimulated dorsal (**B,C**) and ventral (**D,E**) dendrites from one NL neuron imaged at 0 and 4 hours. Images at left were taken at 0 hours. The same dendrites imaged 4 hours later are shown at right. Both sets of dendrites remained fairly stable, but several branches can be observed to retract between the imaging periods (arrows). Scale bar = 20 μm.

time points. Figure 1 shows a representative example of an unstimulated, control NL neuron. There are few obvious changes in the dendrites between the two imaging time points. In contrast, with differential stimulation of the inputs to the dorsal and ventral dendrites, dendritic branches appear much less stable across imaging time points. Dramatic examples of NL neurons that received unilateral stimulation of either their dorsal or their ventral dendrites are shown in Figures 2 and 3, respectively. A qualitative comparison of the initial (0 hours) and final images for both manipulations indicated that many of the stimulated dendrites remained stable between the imaging time points. However, several stimulated branches displayed substantial growth (arrowheads in Figs. 2B,C, 3D,E). Conversely, a number of the unstimulated dendrites in Figures 2D,E and 3B,C appeared to retract in response to the relative deprivation (arrows in images). Unexpectedly, with bilateral stimulation for 4 hours (Fig. 4), both sets of dendrites remained fairly stable over the imaging period, although examples of growing and retracting branches can be observed.

Balanced synaptic input to the two sets of NL dendrites maintains their relative dendritic branch lengths

To quantify the changes in dendritic branch length, total dendritic branch length (TDBL) measurements were made in three-dimensional image stacks at the 0 hours and the 4–5 hours time point. The percentage change in

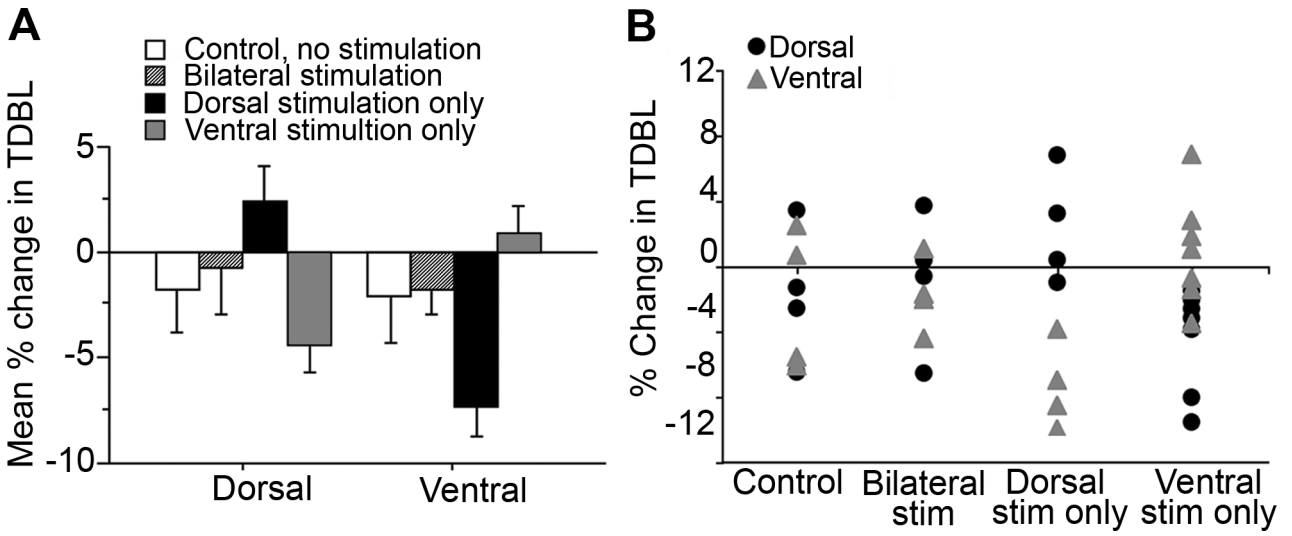

Figure 5. Effect of unstimulated, control, bilateral stimulation and unilateral stimulation conditions on the two sets of NL dendrites. Mean total dendritic branch length (TDBL) was measured separately for the dorsal and ventral dendrites of NL neurons imaged at 0 hours and then again after 4–5 hours for each of the four conditions: the unstimulated control condition, bilateral stimulation, dorsal stimulation, and ventral stimulation. **A:** Bar graph showing the mean percentage change ± SE in TDBL between imaging periods for the control condition and the three stimulation conditions. NL dendrites changed very little in the unstimulated control condition or with bilateral stimulation. With both manipulations, the dorsal and ventral dendrites lost a small amount of TDBL, and there were no significant differences between the two groups or the two sets of dendrites in each group. Differential stimulation of either the dorsal dendrites or the ventral dendrites led to a small increase in the size of the stimulated dendrites and a decrease in the size of the unstimulated dendrites. For each stimulation condition, the two sets of dendrites differed significantly from one another. **B:** Changes in TDBL for individual neurons. Control neurons and bilaterally stimulated neurons exhibited both increases and decreases in dendritic length over the imaging period. However, for each neuron, both sets of dendrites changed in the same direction, either adding or decreasing TDBL. In contrast, with either dorsal or ventral stimulation, all unstimulated dendrites lost TDBL over the imaging period, while the majority of stimulated dendrites increased TDBL.

TDBL between the two imaging periods is shown in Figure 5A. In unstimulated and bilateral stimulation conditions, both the dorsal and the ventral dendrites exhibited a small change in dendritic length during the imaging period. The dorsal dendrites of bilaterally stimulated neurons lost −0.8% ± 2.1% of their length compared with unstimulated, control neurons, which lost −1.7% ± 2.0%. The changes for the ventral dendrites were equally small: −1.8% ± 1.1% for the bilaterally stimulated neurons compared with −2.1% ± 2.2% for control neurons. There were no significant differences for either group in the percentage change in TDBL between imaging time points. These results indicate that, at least on this short time scale, balanced, action-potential-mediated signaling does not induce significant changes in the two sets of NL dendrites beyond that observed for the unstimulated, control condition. It should be noted that the bilateral stimulation condition might be more representative of normal physiological conditions than our unstimulated, "control" neurons, insofar as the inputs from NM fire at high rates even in the absence of sound (Born et al., 1991). It is important to note that there were no differential changes between the dorsal and the ventral dendrites in either the bilateral stimulation condition or the unstimulated, control condition. When we looked at the changes in TDBL for individual neurons (Fig. 5B), we found that half of the neurons in each group had dendrites that grew, whereas the other half had dendrites that lost length. Interestingly, for all neurons analyzed from the unstimulated, control and bilateral stimulation conditions, both sets of dendrites always changed in the same direction, whether this was by adding or by decreasing total dendritic length.

Input-dependent changes in NL dendritic length with differential stimulation of the two sets of dendrites

When we quantitatively compared the mean percentage change in TDBL between the dorsal and the ventral dendrites for the unilateral stimulation conditions at the initial and final imaging time points (Fig. 5A), we found that each set of stimulated dendrites changed significantly relative to the unstimulated dendrites on the opposite side of the cell. Specifically, with selective stimulation of the dorsal dendrites for 4 hours, there was a small, but reliable, increase in TDBL (2.4% ± 1.7%), whereas the unstimulated, ventral dendrites on the

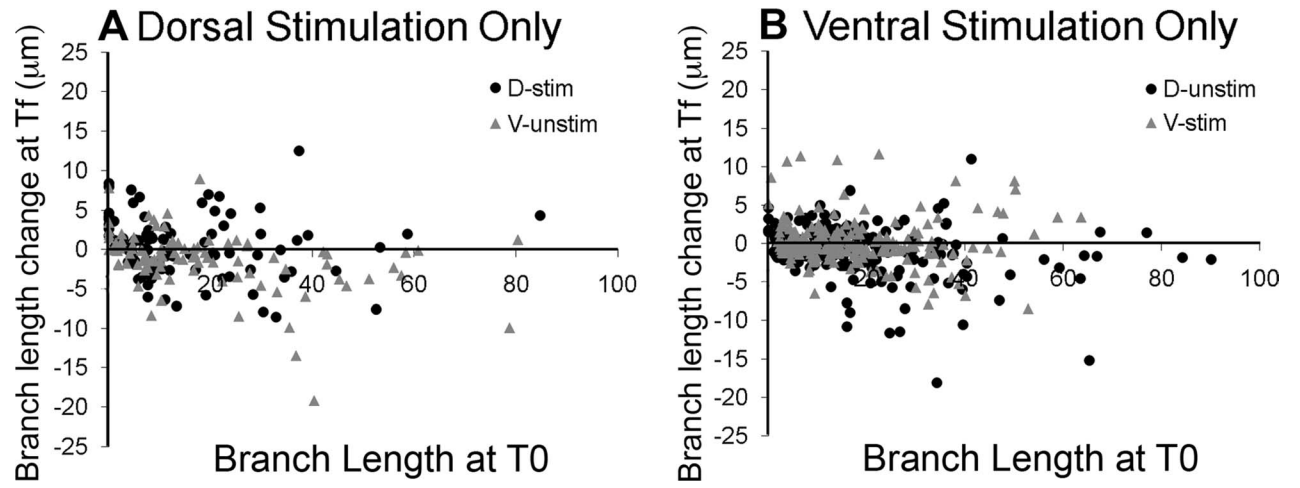

Figure 6. Scatterplot comparisons of the change in individual branch length between 0 and 4–5 hours of live imaging with unilateral stimulation conditions. The initial branch length at 0 hours is indicated on the x-axis, and the amount of length lost or gained at the final time point is indicated on the y-axis. **A:** The branches of differentially stimulated dorsal dendrites (circles) exhibited fairly balanced growth and retraction over the imaging period, although a number of branches grew by 5–10 μm. In contrast, the majority of longer branches (20 μm and above) of unstimulated ventral dendrites (triangles) lost length in response to the relative lack of stimulation (~83%). **B:** The branches of differentially stimulated, ventral dendrites (triangles) exhibited fairly balanced growth and retraction over the imaging period though several branches exhibited large (+10 μm) increases in length. Conversely, the majority of longer branches of unstimulated, dorsal dendrites (circles) exhibited a decrease in branch length over the imaging period (~74%).

opposite side of the same cells lost a larger amount of TDBL (–7.3% ± 1.3%, $P < 0.005$). The losses in TDBL from unstimulated dendrites were also significantly different from the control and bilaterally stimulated ventral dendrites ($P < 0.04$ and $P < 0.03$, respectively). Similarly, with selective stimulation of the ventral dendrites, there was a small, but significant increase in the length of the stimulated ventral dendrites (1.0% ± 1.3%) relative to the decrease in the length of the unstimulated dorsal dendrites, which lost –4.4% ± 1.2% with 4 hours of relative deprivation ($P < 0.01$).

When we looked at TDBL changes for each individual neuron (Fig. 5B), we found that the unstimulated dendrites of all differentially stimulated neurons lost TDBL. The stimulated dendrites of differentially stimulated neurons did not exhibit such a uniform response for either dorsal-only or ventral-only stimulation. However, for the majority of neurons (7 of 11) the stimulated dendrites displayed increases in TDBL, whereas the remaining cells lost only a very small amount of TDBL. These results are quite different from what we found for individual bilaterally stimulated and unstimulated control neurons. For these neurons, the two sets of dendrites either grew or retracted to a similar degree over the imaging period.

For all manipulations, we also compared the initial and final sizes of individual dendritic branches in order to understand how branches of different lengths were affected by our different stimulation conditions. Figure 6A shows all individual dendritic branches from neurons exposed to 4–5 hours of unilateral synaptic stimulation of the dorsal dendrites. For NL neurons, the majority of dendritic branches are smaller than 10 μm. With dorsal-only stimulation, a fairly balanced number of the small branches of unstimulated ventral dendrites grew (~44%) or retracted (~56%) between the imaging time points, whereas the majority (~83%) of longer branches (20 μm and above) lost length over the imaging period. The same was not true for the stimulated dorsal dendrites. For branches of all lengths (including the longest branches), a relatively equal number grew (~49%) and retracted (~51%) during the stimulation period. We obtained similar results when we performed individual branch length analyses on NL neurons that received unilateral synaptic stimulation of their ventral dendrites (Fig. 6B). For the unstimulated, dorsal dendrites, the majority of the longer branches (longer than 20 μm) lost length over the imaging period (~74%), whereas shorter branches grew or retracted in equal numbers. As with dorsal-only stimulation, all branches of stimulated ventral dendrites grew (~42%) and retracted (~58%) to a similar extent. Thus, for both unilateral stimulation conditions, the imbalance of input promotes retraction of the unstimulated branches, particularly branches longer than 20 μm, regardless of the set of dendrites that is deprived.

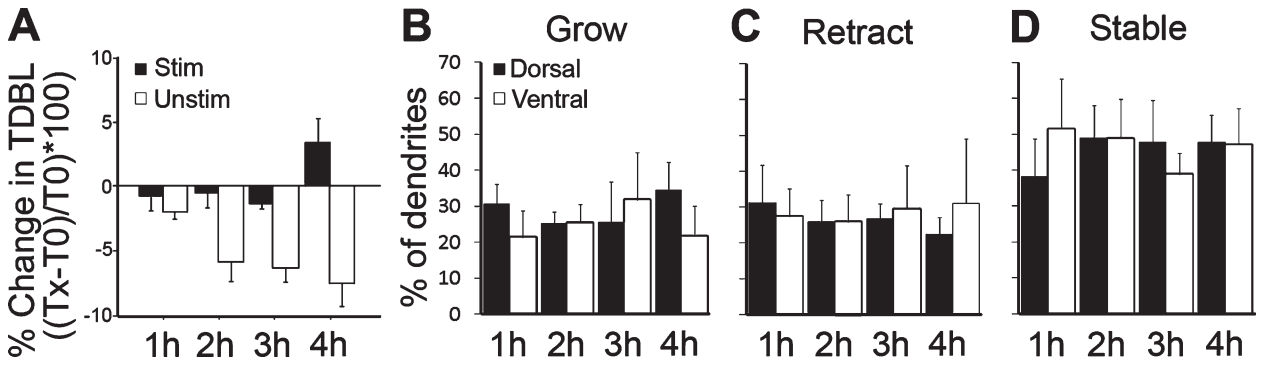

Figure 7. Progressive changes in NL neurons with differential stimulation of the dorsal dendrites. The mean percentage change ± SE between TDBL at 0 hours compared with TDBL at 1, 2, 3, and 4 hours of differential stimulation. **A:** Dorsally stimulated NL neurons exhibited an early decrease in the size of the unstimulated ventral dendrites that was significantly different from the dorsal dendrites after just 2 hours of relative deprivation. TDBL continued to decrease at the 3-hour and 4-hour time points. Growth of the stimulated dorsal dendrites was delayed relative to that of the retraction of the unstimulated ventral dendrites. At the 1–3-hour time points, TDBL changed little, but by 4 hours there was a significant increase in the size of the stimulated dorsal dendrites compared with the unstimulated ventral dendrites. **B–D:** Branch dynamics with dorsal-only stimulation. The bar graphs show the mean percentage of all dendritic branches that grew (B), retracted (C), or remained stable (D) within 10% of their original length ± SE, during the imaging period. For both sets of dendrites, ~50% of the branches remained stable throughout the imaging period, and the remaining ~50% either grew or retracted in relatively equal proportions. Differential stimulation does not significantly alter branch dynamics within the 4-hour time period.

In contrast, few individual branches of bilaterally stimulated or control neurons exhibited large changes in length (data not shown). With these conditions, individual dendritic branches remained fairly stable between imaging time points, and the two sets of dendrites had a relatively equal number of growing and retracting branches. These findings further suggest that balanced input, in the form of either action-potential-mediated signaling (bilateral stimulation) or spontaneous glutamate release (unstimulated, control condition) encourages branch stability and maintains the relative sizes of the two sets of dendrites.

Progressive changes in TDBL with differential stimulation

To assess further the NL dendritic changes over time with unilateral or bilateral synaptic stimulation, we analyzed the percentage change in TDBL each hour during the experimental period. Figure 7A illustrates the time course of changes in NL dendrites with selective stimulation of the dorsal dendrites. With this manipulation, NL neurons exhibited an early decrease in the size of the unstimulated ventral dendrites after just 2 hours of relative deprivation (–5.8% ± 1.5%, $P < 0.05$, relative to 1 hour). This decrease continued at the 3-hour (–6.3% ± 1.1%, $P < 0.03$, relative to 1 hour) and 4-hour (–7.5% ± 1.9%, $P < 0.02$, relative to 1 hour) time points, though at a slower rate of change compared with earlier time points. The change in the stimulated, dorsal dendrites was delayed relative to the unstimulated ventral dendrites. There were no significant differences in the TDBL of the stimulated, dorsal dendrites until the 4-hour time point, when there was a significant increase in the size of the stimulated, dorsal dendrites (3.5% ± 1.9%), compared with all other time points (1 hour: $P < 0.04$, 2 hours: $P < 0.05$, 3 hours: $P < 0.02$). Across the imaging period, the changes in TDBL also differed significantly between the two sets of dendrites (2 hours: $P < 0.04$, 3 hours: $P < 0.01$, 4 hours: $P < 0.02$). These results demonstrate that, with an imbalance of synaptic input, NL dendrites respond by first decreasing the length of their unstimulated dendrites and then increasing the length of their stimulated dendrites.

To determine how branch dynamics changed over the imaging period with dorsal-only stimulation, we quantified the proportion of growing, retracting, and stable branches (these numbers add up to 100%) at each of these time points (Fig. 7B–D). For both sets of dendrites, ~50% of the dendritic branches remained stable over the imaging period, and the remaining 50% grew or retracted in relatively equal proportion. These findings show that the TDBL lost with the relative lack of stimulation likely resulted from decreases in the length of individual branches (particularly branches longer than 20 μm; see Fig. 6) rather than increases in the proportion of retracting dendrites. These results are reflected in the images of dorsal-only stimulation neurons in Figure 2D,E, in which several individual branches of unstimulated ventral dendrites lost substantial length between the two imaging time points.

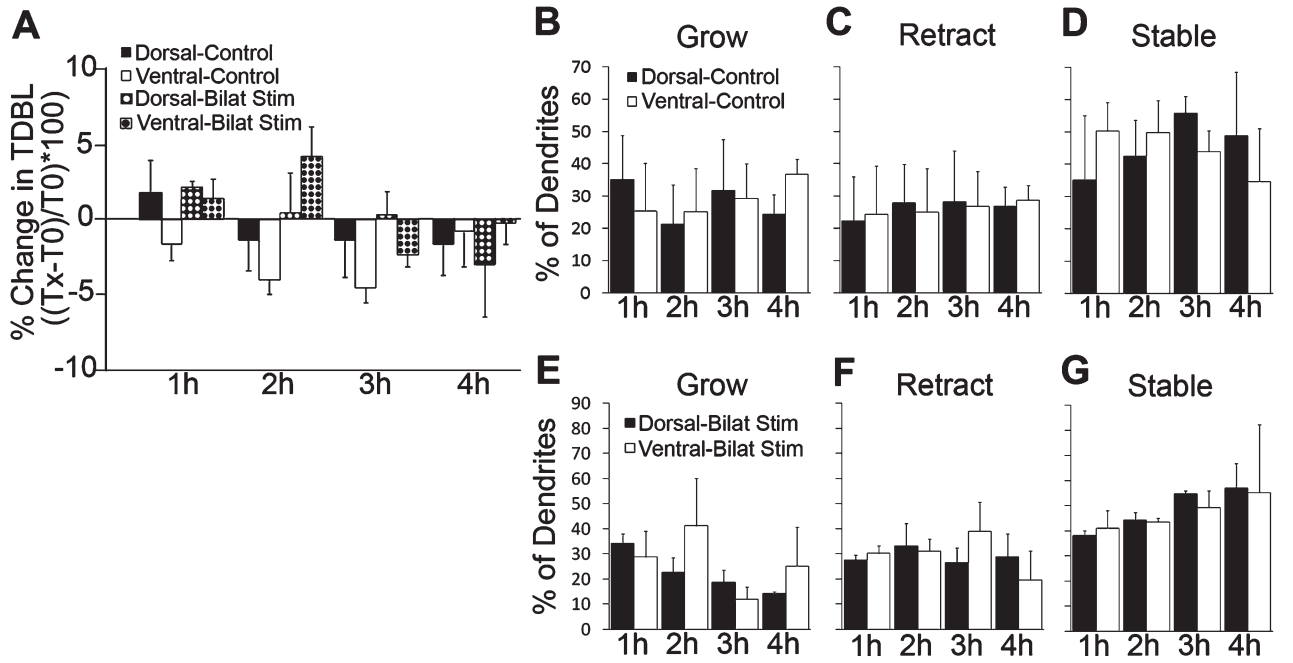

Figure 8. **A:** Progressive changes in NL neurons with the bilateral stimulation or unstimulated control conditions. The mean percentage change ± SE between TDBL at the 0 hours compared with TDBL at the 1-, 2-, 3-, and 4-hour imaging time points. With bilateral stimulation, there were no significant changes in TDBL over the imaging period. The small, initial increase in TDBL of the stimulated dorsal and ventral dendrites at the 1-hour and 2-hour time points was not maintained at 3 hours and 4 hours. In contrast, the ventral dendrites of unstimulated control neurons exhibited a decrease in length at the 2-hour and 3-hour time points, but this decrease was not maintained at 4 hours, and the dorsal dendrites of unstimulated control neurons remained stable throughout the imaging time period. Dynamic changes in individual branches with bilateral stimulation (**B–D**) and unstimulated control (**E–G**) conditions. The bar graphs indicate the mean percentage ± SE of dendritic branches that grew, retracted, or remained stable (within 10% of their original length) during the imaging period. For both the dorsal (d) and the ventral (v) sets of dendrites, for both manipulations, ~50% of the branches remained stable throughout the imaging period, and the remaining ~50% either grew or retracted in relatively equal proportion. However, for the dorsal and ventral dendrites of bilaterally stimulated neurons, there appeared to be a trend toward an increase in the proportion of stable branches over the imaging period. Neither manipulation altered the relative sizes of the two sets of dendrites (bilateral stimulation, n = 2; control, n = 3).

Unlike NL neurons that received selective stimulation of their dorsal dendrites, bilaterally stimulated and unstimulated control NL neurons did not display reliable and continuous differential changes in TDBL over time (Fig. 8A). There were no significant differences in TDBL across the imaging time points for either set of dendrites, with either condition. The dorsal and ventral sets of dendrites changed together, exhibiting increases or decreases in TDBL over the imaging period. Branch dynamics were also fairly similar for the two sets of dendrites under these conditions and reflected the results seen for dorsal-only stimulation of neurons. In both the bilateral stimulation and the unstimulated, control conditions, half of the dorsal and ventral dendritic branches remained stable during the imaging period, whereas the remaining half displayed balanced growth and retraction. Interestingly, we did observe a progressive increase in the proportion of stable branches with bilateral stimulation for both dorsal and ventral dendrites over the imaging period.

When we compared branch dynamics at the initial and final imaging time points for all cells, for all manipulations, a slightly different picture of branch dynamics emerged (Fig. 9). The least amount of dendritic stability was detected for the control dendrites, which grew, retracted, and remained stable in relatively equal proportions (~30%). In contrast, the selectively stimulated dorsal dendrites had a nearly significant increase in the proportion of growing branches (39.6% ± 8.1%) relative to the unstimulated ventral dendrites on the opposite side of the cell (18.0% ± 5.0%, $P = 0.08$). The selectively stimulated ventral dendrites exhibited a decrease in the proportion of retracting branches relative to the unstimulated dorsal dendrites and a surprising increase in the proportion of stable dendrites (48.9% ± 5.3%) relative to growing (26.7% ± 3.0%) and retracting (24.4% ± 5.3%) branches ($P < 0.006$). With this condition, the unstimulated dorsal dendrites on the opposite side of the cell displayed a decrease in the proportion of growing branches (21.0% ±

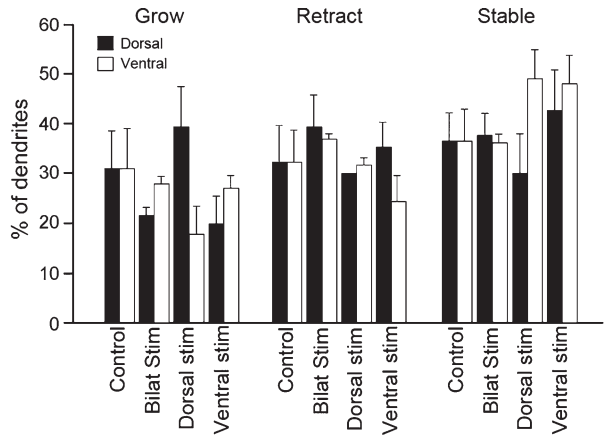

Figure 9. Dynamic changes in individual branches with bilateral stimulation, unilateral stimulation, and unstimulated control conditions. The bar graph indicates the mean percentage ± SE of dendritic branches that grew, retracted, or remained stable (within 10% of their original length) during the imaging period. For both the dorsal and the ventral sets of control dendrites and bilaterally stimulated dendrites, relatively equal proportions of dendrites grew, retracted, and remained stable over the imaging period. For the two differential stimulation conditions, dorsal stimulation and ventral stimulation, ~50% of the dendritic branches remained stable throughout the imaging period, and the remaining ~50% either grew or retracted in relatively equal proportions. However, for the stimulated dorsal dendrites, there was a nearly significant increase in the proportion growing branches compared with the unstimulated ventral dendrites on the opposite side of the cell. Similarly, with ventral-only stimulation, there was a decrease in the proportion of retracting branches for the stimulated ventral dendrites relative to the unstimulated dorsal dendrites on the opposite side of the cell. Both differential stimulation conditions appeared to enhance stability of individual branches relative to the control and bilateral stimulation conditions.

5.2%) relative to the proportion of stable branches (43.4% ± 8.6%, $P < 0.03$). These results suggest that differential synaptic input increases individual branch stability, suppresses branch retraction, and enhances growth of stimulated dendrites relative to unstimulated dendrites on the opposite side of the cell.

In summary, our data show that NL dendrites rapidly respond to relative changes in synaptic input by changing their TDBL; the length of their individual branches; and the proportion of growing, retracting, and stable branches. Furthermore, TDBL appears to be first lost from one dendritic arbor in response to a relative decrease in synaptic input, then added to the other dendritic arbor in response to a relative increase in input.

DISCUSSION

The goal of this study was to understand how the *relative* activity of axonal inputs influences the short-term stability and plasticity of dendritic structure in NL neurons. The symmetry of the two sets of NL dendrites and the segregation of their excitatory inputs allowed us to test this relationship directly. For these experiments, we imaged single, dye-filled NL neurons via two-photon laser scanning microscopy while using electrophysiology to manipulate the amount and pattern of synaptic input to the two sets of dendrites. Input-dependent structural changes in whole sets of dendrites have been suggested by in vivo studies in other systems (for review see Redmond, 2008). For example, in response to behavioral or afferent deprivation, the orientation of dendrites shifts away from inactive afferents, toward active afferents (Katz and Constantine-Paton, 1988; Kossel et al., 1995; Tailby and Metha, 2004). However, these studies were unable to demonstrate whether this change occurred as a result of a physical displacement of existing dendrites or whether existing dendrites were first eliminated and then replaced by new dendrites. Input-dependent dendritic remodeling has been convincingly demonstrated in vitro for small subsets of dendritic spines (Engert and Bonhoeffer, 1999; Maletic-Savatic et al., 1999). However, the spatial and temporal dynamics of input-dependent changes for whole sets of dendrites have not been investigated. By manipulating both the presence and the pattern of input to the two sets of NL dendrites, we were able to demonstrate that relative, but not absolute, input determines dendritic length in NL on a very rapid time scale.

Balanced input maintains the relative sizes of the two sets of dendrites in NL

Simultaneously stimulating the two sets of NL dendrites for 4–5 hours in vitro (bilateral stimulation) led only to small, balanced changes in TDBL and the length of individual branches. In fact, balanced, suprathreshold input to the two sets of dendrites actually increased branch stability over the imaging time points. Similarly, unstimulated, control neurons, which received only subthreshold spontaneous glutamatergic input over the imaging period, also displayed only small changes in TDBL over the imaging period and a relatively high level of branch stability. Previous studies from our laboratory suggested that spontaneous glutamate release is sufficient for maintaining NL dendrites under control conditions in vitro (Sorensen and Rubel, 2006). Surprisingly, the higher level of balanced, glutamatergic input induced by bilateral stimulation also appears to maintain dendritic length in NL (at least over this short time scale).

Although we hypothesized that the pattern of synaptic input would be critical for regulating the relative sizes of NL dendrites, we also thought that an overall increase in

action-potential-mediated (APM) signaling beyond control conditions might promote growth of both sets of stimulated dendrites. Although in many sensory systems APM signaling is not required for dendrite development (Rajan and Cline, 1998; Rajan et al., 1999; Wong et al., 2000), elevated glutamatergic input and/or KCl induced depolarization has been found to promote dendritic outgrowth (Vaillant et al., 2002). Experimental limitations might have prevented us from fully testing the effect of balanced APM input on the regulation of NL dendrites in the current studies. Specifically, these experiments were relatively short, lasting for only 4–5 hours. A longer period of stimulation may be required to promote stable dendritic growth in this system. Additionally, the frequency of stimulation we used to activate NL dendrites (10–25 Hz) might have enhanced their maintenance rather than their growth. In the hippocampus, very low (1 Hz) and high (100 Hz) stimulation rates have dramatically different effects on dendrite structure. High-frequency stimulation induces growth of dendritic spines, whereas low-frequency stimulation promotes spine loss (Nagerl et al., 2004; Zhou et al., 2004) and stabilization of dendritic shafts (Lin et al., 2005).

The pattern of synaptic input regulates the relative sizes of the two sets of NL dendrites

In contrast to the bilateral stimulation and control conditions, in response to selective stimulation of the dorsal dendrites we saw an increase (~3–4%) in the size of the stimulated dorsal dendrites and a significant decrease (~7.5%) in the size of the unstimulated ventral dendrites. This result supports our previous findings on slightly older NL neurons (Sorensen and Rubel, 2006). Moreover, when we selectively stimulated ventral NL dendrites, we also found a small increase in the size of stimulated dendrites and a significant decrease (~4.5%) in the size of the unstimulated dorsal dendrites on the opposite side of the cell. These findings demonstrate that relative synaptic input regulates both sets of dendrites, regardless of which set is differentially activated.

For both unilateral manipulations (dorsal only and ventral only stimulation), we also saw large changes (~75–85%) in the percentage of longer dendritic branches that exhibited losses in branch length in response to relative deprivation. This finding is somewhat unusual. Activity-dependent branch length changes are typically observed for shorter, terminal branches (Sin et al., 2002). However, at this developmental age, branch length in NL neurons is being altered across the entire dendritic arbor (Smith, 1981; Smith and Rubel, 1979). This finding might suggest that during development longer dendrites, such as primary dendrites, are the regions of NL neurons that integrate changes (particularly losses) in presynaptic inputs by altering their morphology. On the other hand, stimulated dendrites displayed either increases in the proportion of growing branches (stimulated dorsal) or decreases in the proportion of retracting branches (stimulated ventral) in response to differential stimulation. However, these changes were small. Thus it is likely that moderate changes in the length of individual dendritic branches, along with more modest changes in the proportion of growing and retracting branches, underlie the changes in TDBL observed for the two sets of NL dendrites with differential stimulation.

To understand the time course over which the two sets of differentially stimulated dendrites respond to changes in presynaptic input, we also analyzed TDBL and branch dynamics once per hour throughout the 4 hours of dorsal-only stimulation. We found that retraction of the unstimulated dendrites preceded growth of the stimulated dendrites by several hours. These results suggest that, in NL, dendritic branch length can rapidly shift from inactive dendrites to active dendrites. This is one of the first demonstrations of localized, input-dependent changes in whole sets of dendrites in which losses of membrane surface from inactive dendrites appear to be replaced by additions to active dendrites in the same neuron within a very short period. It is unclear from our current work whether membrane is actively transferred from one set of dendrites to the other or whether the membrane losses and additions result from distinct but coordinated processes. Activity-dependent endo- and exocytosis could lead to changes in membrane surface area (Kennedy et al., 2010; Newpher and Ehlers, 2009; Peebles et al., 2010), but targeted, activity-dependent trafficking of membrane remains to be investigated.

Inter- and intracellular mechanisms regulating NL dendrites

So far, the intracellular signaling cascades underlying dendritic regulation by afferent input have not been fully elucidated. This process could be mediated by a limited distribution of 1) "maintenance or growth" signals (Van Aelst and Cline, 2004; Wong and Ghosh, 2002) and/or 2) "retraction" signals (Fu et al., 2007; Hata et al., 1999; Mironov et al., 2009) found throughout the neuron. Putative maintenance/growth signals that have been suggested by experiments in other systems include neurotrophins, glutamate, and intracellular calcium (Lohmann and Wong, 2005; McAllister et al., 1996, 1997; Redmond, 2008). In our system, maintenance of NL dendrites requires glutamatergic input (Sorensen and Rubel, 2006). Glutamate-induced, intracellular calcium signaling might function as both a maintenance/growth and a retraction

signal capable of communicating relative changes in synaptic strength between the two sets of NL dendrites. In other systems, local calcium release from internal stores is known to influence dendritic stability (Lohmann et al., 2002). In this study, the unilateral stimulation protocol that alters dendritic stability also induces rapid and differential changes in intracellular calcium signaling within each set of NL dendrites [S.A.S, unpublished personal observation, but see Blackmer et al. (2009) for the calcium response to individual action potentials]. Locally regulated calcium signaling has also been observed in vivo in other developing sensory systems in response to physiological stimuli (Bollman and Engert, 2009). Local changes in calcium signaling can alter the activation of kinases and transcriptional regulators (Wong and Ghosh, 2002) and influence gene expression (Flavell and Greenberg, 2008; Redmond and Ghosh, 2005) as well as the expression and localization of glutamate receptors (Martin and Henley, 2004; Wang et al., 2009) and cytoskeletal elements (Ciani and Salinas; Luo, 2002; Okamoto et al., 2004; Zheng and Poo, 2007), all of which can shape dendritic form. In NL, cytoskeletal changes are known to accompany deafferentation- and deprivation-induced losses in dendrite structure (Deitch and Rubel, 1989; Wang and Rubel, 2008), and rapid changes in calcium regulatory proteins have also been observed (Wang et al., 2009). On this short time scale, the relative decrease in activity in the unstimulated dendrites could lead to calcium-regulated destabilization of the cytoskeleton, resulting in a local, rapid loss in dendritic length. The slower time scale associated with growth of the stimulated dendrites may result from the increased time required to have additional proteins and membrane synthesized and/or shipped to the correct location. Studies combining electrophysiology, pharmacology, and time-lapse calcium imaging will help to identify the intracellular signals involved in differentially regulating NL dendrite structure.

Another important possibility to consider is whether the dendritic remodeling observed in these studies occurred in response to intercellular, rather than intracellular, signals (Cline and Haas, 2008; Haas et al., 2006). Specifically, our differential stimulation protocol might have induced structural or functional changes in the presynaptic inputs to NL. In other systems, depolarization-enhanced growth of stimulated axons has been shown to initiate the degradation of less active inputs to the same neurons (Singh and Miller, 2005). In this scenario, unstimulated NL dendrites may lose TDBL in response to degeneration or complete inactivation of their unstimulated presynaptic terminals, whereas stimulated terminals and their postsynaptic dendrites either grow or are maintained. Indeed, in this system, input-dependent changes in calcium regulation within presynaptic terminals have been suggested (Wang et al., 2009). Simultaneous imaging of pre- and postsynaptic structures will shed light on whether presynaptic changes facilitate and/or accompany changes in postsynaptic structure in NL.

ACKNOWLEDGMENTS

We thank Glen MacDonald for expert imaging advice and writing Object Image macros, Kevin Witham for computer expertise, Dr. Nigel Bamford for the generous loan of his electrophysiology and related imaging equipment, and the UW department of Ophthalmology for use of the multi-photon imaging facilities.

LITERATURE CITED

Balice-Gordon RJ, Lichtman JW. 1994. Long-term synapse loss induced by focal blockade of postsynaptic receptors. Nature 372:519–524.

Benes FM, Parks TN, Rubel EW. 1977. Rapid dendritic atrophy following deafferentation: an EM morphometric analysis. Brain Res 122:1–13.

Blackmer T, Kuo SP, Bender KJ, Apostolides PF, Trussell LO. 2009. Dendritic calcium channels and their activation by synaptic signals in auditory coincidence detector neurons. J Neurophysiol 102:1218–1226.

Bollman JH, Engert F. 2009. Subcellular topography of visually driven activity in the vertebrate visual system. Neuron 61: 813–814.

Born DE, Durham D, Rubel EW. 1991. Afferent influences on brainstem auditory nuclei of the chick: nucleus magnocellularis neuronal activity following cochlea removal. Brain Res 557:37–47.

Carr CE, Konishi M. 1990. A circuit for detection of interaural time differences in the brain stem of the barn owl. J Neurosci 10:3227–3246.

Ciani L, Salinas PC. 2008. From neuronal activity to the actin cytoskeleton: a role for CaMKKs and βPIX in spine morphogenesis. Neuron 57:3–4.

Cline H, Haas K. 2008. The regulation of dendritic arbor development and plasticity by glutamatergic synaptic input: a review of the synaptotrophic hypothesis. J Physiol 586: 1509–1517.

Deitch JS, Rubel EW. 1984. Afferent influences on brain stem auditory nuclei of the chicken: time course and specificity of dendritic atrophy following deafferentation. J Comp Neurol 229:66–79.

Deitch JS, Rubel EW. 1989. Rapid changes in ultrastructure during deafferentation-induced dendritic atrophy. J Comp Neurol 281:234–258.

Engert F, Bonhoeffer T. 1999. Dendritic spine changes associated with hippocampal long-term synaptic plasticity. Nature 399:66–70.

Feng AS, Rogowski BA. 1980. Effects of monaural and binaural occlusion on the morphology of neurons in the medial superior olivary nucleus of the rat. Brain Res 189: 530–534.

Flavell SW, Greenberg ME. 2008. Signaling mechanisms linking neuronal activity to gene expression and plasticity of the nervous system. Annu Rev Neurosci 31:563–590.

Fu WY, Chen Y, Sahin M, Zhao XS, Shi L, Bikoff JB, Lai KO, Yung WH, Fu AK, Greenberg ME, Ip NY. 2007. Cdk5 regulates EphA4-mediated dendritic spine retraction through an ephexin1-dependent mechanism. Nat Neurosci 10:67–76.

Gao H, Lu Y. 2008. Early development of intrinsic and synaptic properties of chicken nucleus laminaris neurons. Neuroscience 153:131–143.

Haas K, Sin WC, Javaherian A, Li Z, Cline HT. 2001. Single-cell electroporation for gene transfer in vivo. Neuron 29: 583–591.

Haas K, Li J, Cline HT. 2006. AMPA receptors regulate experience-dependent dendritic arbor growth in vivo. Proc Natl Acad Sci U S A 103:12127–12131.

Hashimoto K, Ichikawa R, Kitamura K, Watanabe M, Kano M. 2009. Translocation of a "winner" climbing fiber to the Purkinje cell dendrite and subsequent elimination of "losers" from the soma in developing cerebellum. Neuron 63:106–118.

Hata Y, Tsumoto T, Stryker MP. 1999. Selective pruning of more active afferents when cat visual cortex is pharmacologically inhibited. Neuron 22:375–381.

Hua JY, Smear MC, Baier H, Smith SJ. 2005. Regulation of axon growth in vivo by activity-based competition. Nature 434:1022–1026.

Katz LC, Constantine-Paton M. 1988. Relationships between segregated afferents and postsynaptic neurones in the optic tectum of three-eyed frogs. J Neurosci 8:3160–3180.

Katz LC, Shatz CJ. 1996. Synaptic activity and the construction of cortical circuits. Science 274:1133–1138.

Kennedy MJ, Davison IG, Robinson CG, Ehlers MD. 2010. Syntaxin-4 defines a domain for activity-dependent exocytosis in dendritic spines. Cell 141:524–535.

Kossel A, Lowel S, Bolz J. 1995. Relationships between dendritic fields and functional architecture in striate cortex of normal and visually deprived cats. J Neurosci 15: 3913–3926.

Lichtman JW, Colman H. 2000. Synapse elimination and indelible memory. Neuron 25:269–278.

Lin B, Kramar EA, Bi X, Brucher FA, Gall CM, Lynch G. 2005. Theta stimulation polymerizes actin in dendritic spines of hippocampus. J Neurosci 25:2062–2069.

Lohmann C, Wong RO. 2005. Regulation of dendritic growth and plasticity by local and global calcium dynamics. Cell Calcium 37:403–409.

Lohmann C, Myhr KL, Wong RO. 2002. Transmitter-evoked local calcium release stabilizes developing dendrites. Nature 418:177–181.

Luo L. 2002. Actin cytoskeleton regulation in neuronal morphogenesis and structural plasticity. Annu Rev Cell Dev Biol 18:601–635.

Maletic-Savatic M, Malinow R, Svoboda K. 1999. Rapid dendritic morphogenesis in CA1 hippocampal dendrites induced by synaptic activity. Science 283:1923–1927.

Martin S, Henley JM. 2004. Activity-dependent endocytic sorting of kainate receptors to recycling or degradation pathways. EMBO J 23:4749–4759.

McAllister AK, Katz LC, Lo DC. 1996. Neurotrophin regulation of cortical dendritic growth requires activity. Neuron 17: 1057–1064.

McAllister AK, Katz LC, Lo DC. 1997. Opposing roles for endogenous BDNF and NT-3 in regulating cortical dendritic growth. Neuron 18:767–778.

Mironov SL, Skorova E, Hartelt N, Mironova LA, Hasan MT, Kugler S. 2009. Remodelling of the respiratory network in a mouse model of Rett syndrome depends on brain-derived neurotrophic factor regulated slow calcium buffering. J Physiol 587:2473–2485.

Monsivais P, Yang L, Rubel EW. 2000. GABAergic inhibition in nucleus magnocellularis: implications for phase locking in the avian auditory brainstem. J Neurosci 20:2954–2963.

Nagerl UV, Eberhorn N, Cambridge SB, Bonhoeffer T. 2004. Bidirectional activity-dependent morphological plasticity in hippocampal neurons. Neuron 44:759–767.

Newpher TM, Ehlers MD. 2008. Glutamate receptor dynamics in dendritic microdomains. Neuron 58:472–497.

Okamoto K, Nagai T, Miyawaki A, Hayashi Y. 2004. Rapid and persistent modulation of actin dynamics regulates postsynaptic reorganization underlying bidirectional plasticity. Nat Neurosci 7:1104–1112.

Parks TN. 1981. Morphology of axosomatic endings in an avian cochlear nucleus: nucleus magnocellularis of the chicken. J Comp Neurol 203:425–440.

Parks TN, Jackson H, Conlee JW. 1987. Axon-target cell interactions in the developing auditory system. Curr Top Dev Biol 21:309–340.

Peebles CL, Yoo J, Thwin MT, Palop JJ, Noebels JL, Finkbeiner S. 2010. Arc regulates spine morphology and maintains network stability in vivo. Proc Natl Acad Sci U S A 107: 18173–18178.

Personius KE, Balice-Gordon RJ. 2001. Loss of correlated motor neuron activity during synaptic competition at developing neuromuscular synapses. Neuron 31:395–408.

Rajan I, Cline HT. 1998. Glutamate receptor activity is required for normal development of tectal cell dendrites in vivo. J Neurosci 18:7836–7846.

Rajan I, Witte S, Cline HT. 1999. NMDA receptor activity stabilizes presynaptic retinotectal axons and postsynaptic optic tectal cell dendrites in vivo. J Neurobiol 38:357–368.

Rebillard G, Rubel EW. 1981. Electrophysiological study of the maturation of auditory responses from the inner ear of the chick. Brain Res 229:15–23.

Redmond L. 2008. Translating neuronal activity into dendrite elaboration: signaling to the nucleus. Neurosignals 16: 194–208.

Redmond L, Ghosh A. 2005. Regulation of dendritic development by calcium signaling. Cell Calcium 37:411–416.

Rubel EW, Smith ZD, Steward O. 1981. Sprouting in the avian brainstem auditory pathway: dependence on dendritic integrity. J Comp Neurol 202:397–414.

Russell FA, Moore DR. 1999. Effects of unilateral cochlear removal on dendrites in the gerbil medial superior olivary nucleus. Eur J Neurosci 11:1379–1390.

Saunders JC, Gates GR, Coles RB. 1974. Brain-stem evoked responses as an index of hearing thresholds in one-day-chicks and ducklings. J Comp Physiol Psychol 86:426–431.

Sin WC, Haas K, Ruthazer ES, Cline HT. 2002. Dendrite growth increased by visual activity requires NMDA receptor and Rho GTPases. Nature 419:475–480.

Singh KK, Miller FD. 2005. Activity regulates positive and negative neurotrophin-derived signals to determine axon competition. Neuron 45:837–845.

Smith DJ, Rubel EW. 1979. Organization and development of brain stem auditory nuclei of the chicken: dendritic gradients in nucleus laminaris. J Comp Neurol 186:213–239.

Smith ZD. 1981. Organization and development of brain stem auditory nuclei of the chicken: dendritic development in N. laminaris. J Comp Neurol 203:309–333.

Sorensen SA, Rubel EW. 2006. The level and integrity of synaptic input regulates dendrite structure. J Neurosci 26: 1539–1550.

Tailby C, Metha A. 2004. Artificial scotoma-induced perceptual distortions are orientation dependent and short lived. Vis Neurosci 21:79–87.

Vaillant AR, Zanassi P, Walsh GS, Aumont A, Alonso A, Miller FD. 2002. Signaling mechanisms underlying reversible, activity-dependent dendrite formation. Neuron 34:985–998.

Van Aelst L, Cline HT. 2004. Rho GTPases and activity-dependent dendrite development. Curr Opin Neurobiol 14: 297–304.

Wang Y, Rubel EW. 2008. Rapid regulation of microtubule-associated protein 2 in dendrites of nucleus laminaris of

the chick following deprivation of afferent activity. Neuroscience 154:381–389.

Wang Y, Cunningham DE, Tempel BL, Rubel EW. 2009. Compartment-specific regulation of plasma membrane calcium ATPase type 2 in the chick auditory brainstem. J Comp Neurol 514:624–640.

Wong RO, Ghosh A. 2002. Activity-dependent regulation of dendritic growth and patterning. Nat Rev Neurosci 3: 803–812.

Wong WT, Faulkner-Jones BE, Sanes JR, Wong RO. 2000. Rapid dendritic remodeling in the developing retina: dependence on neurotransmission and reciprocal regulation by Rac and Rho. J Neurosci 20:5024–5036.

Zheng JQ, Poo MM. 2007. Calcium signaling in neuronal motility. Annu Rev Cell Dev Biol 23:375–404.

Zhou Q, Homma KJ, Poo MM. 2004. Shrinkage of dendritic spines associated with long-term depression of hippocampal synapses. Neuron 44:749–757.